

Binding of Harvested Bacterial Exopolymers to the Surface of Calcite

THOMAS D. PERRY, IV,^{*,†}
 VANJA KLEPAC-CERAJ,[‡]
 XIANG V. ZHANG,[†]
 CHRISTOPHER J. MCNAMARA,[†]
 MARTIN F. POLZ,[‡] SCOT T. MARTIN,[†]
 NEAL BERKE,[§] AND RALPH MITCHELL[†]

Harvard University, Division of Engineering and Applied Sciences, Cambridge, Massachusetts 02138, Massachusetts Institute of Technology, Cambridge, Massachusetts 02139, and W. R. Grace Corporation, Cambridge, Massachusetts 02140

Biologically produced exopolysaccharides (EPS) affect calcite dissolution and precipitation. In this study, natural alkaliphilic microbial isolates were collected from biofilms on historic limestone. The isolates were screened for their ability to produce significant quantities of EPS in cultures. The most productive isolates were identified by 16S rRNA sequence analysis as a close relative of *Bacillus cereus*. EPS with different chemical structures were harvested from the isolates. Isothermal titration calorimetry (ITC) was used to quantify the thermodynamics of binding by the harvested EPS to calcite. The binding was described by a Langmuir adsorption isotherm. Characterization of the EPS showed that binding strength to calcite depended on the chemical nature of the polymer.

Introduction

Dissolution of calcium carbonate (calcite) affects global carbon cycling (1), the chemistry of marine systems (2), the porosity and heterogeneity of aquifers (3), the local pH and alkalinity of natural waters in terrestrial environments (4), and the fate and transport of anthropogenic pollutants, especially heavy metals (5). Additionally, many stone cultural heritage materials are composed predominantly of calcium carbonate in the form of limestone or marble. Retardation of deterioration is important for preserving these artifacts (6). The most important chemical controls of weathering rates are the local pH conditions and the concentration of chelating ligands (7). Although the effect of pH on calcium carbonate dissolution is well-studied (as reviewed in ref 8), the effect of biologically produced ligands is less well-understood.

Biofilms are a rich source of biological ligands. Mature biofilms on mineral surfaces are temporally, spatially, and taxonomically dynamic communities of microorganisms that can affect dissolution through the production of metabolic byproducts. Bacteria, *Archaea*, algae, fungi, and lichens increase calcite dissolution rates through the production of metabolic byproducts, such as organic and inorganic acids

(9–11). Other complex biologically derived compounds, including lipids and phospholipids (12, 13), proteins (12), humics (14), and other carboxylated compounds (15, 16), inhibit dissolution (17,18).

Exopolysaccharide (EPS) is a particularly important class of biological ligands, which biofilm bacteria produce in large amounts. EPS molecules bind minerals and affect the dissolution rate. EPS is generally composed of a variety of sugars often containing functional groups (such as carboxylic acids) that can interact with mineral ions, such as iron or aluminum (19). The chemical structure of EPS is genotypically, phenotypically, and environmentally regulated. It varies by microorganism, growth stage, nutrient abundance, and various environmental stimuli (9). EPS binds to minerals with different strengths, and the complex nature of the EPS–mineral interaction arises from the detailed chemical compositions of EPS and mineral surfaces. The specific dissolution effects of EPS depend on mineral type, ligand functionality, acidic moieties, and pH.

EPS acts by several mechanisms (20), such as by decreasing aqueous saturation through secondary precipitation or by chelating dissolution-inhibiting ions (21). Different types of EPS have been observed to either accelerate or slow mineral dissolution rates (17, 22). However, how these mechanisms and reactions precisely work is not well-established (22–24). We have previously shown that a model, commercially available microbial polysaccharide produced by ubiquitous microorganisms accelerates calcite dissolution by a crystallographically specific, surface-chelation mechanism (21). Quantification of the EPS–mineral interaction is, however, challenging due to the difficulty of retrieving EPS from natural microbial isolates and the chemical complexity of the interactions.

In this study, calcite binding by microbial EPS was investigated by isothermal titration calorimetry (ITC). ITC is a thermodynamic technique that quantifies the heat absorbed or released during chemical reactions. The evolved heat flux is proportional to the amount of binding and can be used to calculate thermodynamic parameters, such as enthalpies of binding. Building on the work by Dimova et al. (25), we utilized ITC to quantify calcite binding by EPS produced by natural microbial isolates. Two EPS-producing microorganisms were collected from stone surfaces and phylogenetically profiled. Additionally, a known calcareous-mineral precipitating microorganism, *Proteus mirabilis*, was investigated. EPS was produced in cultures and chemically characterized. Calcite binding by our collected polymers was measured using ITC, and the data were compared to binding by humic acid. A Langmuir adsorption isotherm (25) thermodynamic model of binding of surficial cations described the EPS–mineral reaction.

Materials and Methods

Sample Collection and Organism Isolation and Identification. The microbial samples were collected from the dark interior of Tomb 25, Athienou Archaeological Project, Mal-loura, Cyprus. The microorganisms were removed from the stone surface by swabbing using a Q-tip in a sterile solution of saline (0.85% NaCl) and dilute (<0.1%) nontoxic surfactant (Triton X-1000) in deionized water. Collected organisms were released into suspension by vortexing and were enriched for alkaliphilic organisms by inoculating the suspensions on a solid alkaliphilic growth medium modified from Horikoshi (26) set to pH 10.5 and allowed to grow at room temperature (23 °C). The medium consisted of 10 g of dextrose, 7 g of NaHCO₃, 10 g of polypeptone, 10 g of yeast extract, 1 g of

* Corresponding author phone: (617)495-4180. Fax: (617)496-1471. E-mail: tperry@deas.harvard.edu.

[†] Harvard University.

[‡] Massachusetts Institute of Technology.

[§] W. R. Grace Corporation.

KH₂PO₄, 0.2 g of Mg₂SO₄·7H₂O, and 20 g of agar in 1 L of water. The dextrose and NaHCO₃ each were prepared in separate 100 mL flasks to prevent hydrolysis. Each solution was adjusted to the desired pH, autoclaved, and combined after cooling. Pure bacterial cultures were obtained by repeated streaking. Several isolates were screened for their ability to produce polymers at high pH values, and one isolated organism (identified as isolate G3) was chosen for further experimentation. The isolated organism *MEX244.1* was selected from a library of microorganisms collected from the Acropolis at the Maya site at Ek' Balam, Yucatan, Mexico, as described in McNamara et al. (27) and enriched under alkaline conditions using a medium containing precipitated calcium carbonate (28).

The selected isolates were identified by 16S rRNA gene sequencing. DNA was extracted using the UltraClean Soil DNA Kit (MoBio Labs, Carlsbad, CA). A portion of the 16S rDNA genes was amplified using the primers 27f and 1492r (29) in PCR protocol (30) carried out in a Robocycler (Stratagene, La Jolla, CA) for 35 cycles under the following conditions: initial denaturation at 94 °C for 3 min, followed by 15 cycles of denaturation at 94 °C for 1 min, primer annealing at 50 °C for 1 min, and elongation at 72 °C for 2 min with a final extension step at 72 °C for 5 min. PCR reactions were conducted in 50 µL volumes and contained 25 pmol of each primer, 0.2 mM dNTP, 5.0 µL of 10x PCR buffer (200 mM Tris-HCl, pH 8.4, 500 mM KCl), 2 mM MgCl₂, 2 U of Taq DNA polymerase (Invitrogen, Carlsbad, CA), 4 µL of template DNA from the extractions, and Nanopure deionized water (18.3 MΩ cm; Barnstead, Dubuque, IA). The amplified fragments were precipitated using a QIAquick PCR purification kit (Qiagen, Valencia, CA) and resuspended. The fragments served as the template for the sequencing PCR reaction using three primers to obtain complete sequences: 27f, 907r, 1942r (29), and a BigDye Terminator kit (Applied Biosystems, Foster City, CA).

16S rRNA gene sequences were edited and assembled using the Sequencher software (Gene Codes) and were checked for quality by manually mapping to a secondary structure of *Bacillus cereus* 16S rRNA (31, 32). Related sequences were identified by comparing sequences against Genbank (33) and by searching against the Ribosomal Database Project (RDP) (34, 35). Phylogenetic analyses were conducted in PAUP, version 4.0b10 (36). Relationships were determined using the neighbor-joining method with Jukes-Cantor correction and checked for consistency using parsimony and maximum likelihood methods. Almost the full length of the sequences (*Escherichia coli* positions 98–1460) was used in the phylogenetic analyses. For each analysis, bootstrap resampling with minimum evolution method with 1000 replicates was used to test robustness.

Polymer Production and Characterization. EPS was produced by growing the isolates in a 15 L batch reactor in nutrient broth with constant stirring and aeration for 96 h at 23 °C. Cells were removed from the culture by tangential filtration through a 0.22 µm membrane filter (Durapore, Pellicon-2, Millipore). The EPS was concentrated 100× using a 5 kD membrane filter (PLCCC, Pellicon-2, Millipore). Contaminating macromolecules, including DNA, RNA, and proteins, were removed by the method of Gonçalves et al. (37). Contaminating salts were removed by centrifugal filtration (10 kD Macrosep filter; Pall, East Hills, NY) and repeated rinsing of EPS retentate with Nanopure water. This protocol resulted in purified polysaccharides.

Collected polymers were characterized by the Complex Carbohydrate Research Center (University of Georgia, Athens, GA). Glycosyl composition and linkage analysis were analyzed using gas chromatography/mass spectrometry (GC-MS) (38) of partially methylated alditol acetates (39). The EPS molecular weights were determined by size-exclusion chro-

matography. A 1 mg sample of a 10 mg mL⁻¹ EPS solution was injected onto a Superose 12 column at a flow rate of 0.40 mL min⁻¹ in 50 mM ammonium formate at pH 4.8. Dextran standards of 10, 40, 67, and 167 kD were run in tandem with the sample.

Isothermal Titration Calorimetry. Calcite crystals (CaCO₃) were prepared by slow crystallization using the technique of Kitano et al. (25, 40). A solution in equilibrium with calcite and 1 atm of CO₂ of calcium carbonate was prepared by bubbling CO₂ gas through a suspension of 5 g of CaCO₃ in 4 L of Nanopure water for 60 min with constant stirring at room temperature. Undissolved CaCO₃ was removed by vacuum filtration through #4 (20–25 µm) Whatman filter paper (Middlesex, UK). Bubbling for another 30 min dissolved any remaining particles in the filtered solution. The solution was stored in an unsealed container and allowed to equilibrate with atmospheric CO₂ (360 ppm) for 48 h at room temperature, during which time calcite precipitated (41). Crystals with well-defined rhombohedral morphology and surface area precipitated after the solution was left. The crystal surface area was quantified by the BET method, which measured gaseous pressure drop as nitrogen/helium/krypton mixtures were sorbed to the crystal surface. The surface area measurements were consistent with optical microscopy measurements (Olympus BX-60, Melville, NY) of a large sample set using transmitted light at 100×. A perfect crystal without meso- or atomic-scale topographical irregularities was assumed in the optical microscopy calculations (42, 43).

Solutions of pure ionic calcium were prepared by filtration (0.1 µm, VC grade; Millipore, Billerica, MA) of the calcite suspensions (25). The absence of large crystals was confirmed by optical microscopy. Although a 0.1 µm pore size was used for filtration, meso-scale calcite aggregations may have still been present in solution (25). The solution calcium concentration was measured using flame atomic absorption spectroscopy.

Interactions of EPS with aqueous calcium cations (Ca_(aq)²⁺) and particulate calcite (CaCO_{3(s)}) interactions were investigated using a VP-ITC calorimeter (MicroCal, Northampton, MA). Solutions were made with Nanopure water, previously degassed for 5 min under vacuum. Experiments were performed at a working volume of 1.428 mL, 30 °C, and a stir rate of 280 rpm to obviate settling of the crystals. Titrations of the 1% (w/w) EPS into deionized water, CaCO_{3(s)} suspension, or Ca_(aq)²⁺ solutions were performed in 10 µL aliquots injected over 20 s with 300 s between injections. An equilibration time of 300 s was necessary to return to baseline, presumably because of sluggish EPS binding kinetics. Analysis of the data was performed using Origin 7.0 (MicroCal).

Results and Discussion

Microorganisms and Polymer Characterization. EPS producing isolates were chosen from libraries of biofilm-forming microorganisms collected from two mineral surfaces based on their viability in alkaline conditions (10 < pH < 12) and their ability to produce EPS. The culture conditions were selected to favor the *Bacillus* genus because several members have been demonstrated to be alkaliphilic (26, 44, 45). The ability of these organisms to grow in high pH environments may be a consequence of the protective strategies of Gram-positive bacteria, such as the presence of neutralizing membrane-bound sodium pumps (46).

The mineral substrate was predominantly calcite. The Cyprus sample was 95% biomicritic calcium carbonate as determined by thin-section polarized light microscopy (47). The Mexico sample was 98% calcite as detailed in ref 48. An isolate that produced significant quantities of EPS in culture was designated G3 and chosen for future experimentation from a pool of over 20 alkaliphilic microorganisms collected

TABLE 1. Glycosyl Composition Analysis

glycosyl residue	G3 EPS		MEX244.1 EPS		<i>P. mirabilis</i> EPS	
	mass (μg)	mol % ^a	mass (μg)	mol % ^a	mass (μg)	mol % ^a
arabinose (Ara)	3.1	5.0	7.4	9.4	15.6	16.3
rhamnose (Rha)	trace	n.d. ^b	2.8	3.2	3.4	3.3
fucose (Fuc)	n.d.	n.d.	n.d.	n.d.	n.d.	n.d.
xylose (Xyl)	2.1	3.4	4.4	5.6	4.9	5.1
glucuronic acid (GlcA)	n.d.	n.d.	n.d.	n.d.	n.d.	n.d.
galacturonic acid (GalA)	trace	n.d.	7.6	7.5	10.3	8.3
mannose (Man)	51.8	70.3	49.2	52.2	35.5	30.6
galactose (Glc)	9.0	12.1	15.9	16.9	26.5	23.0
glucose (Glc)	3.5	4.7	4.9	5.2	15.4	13.4
<i>N</i> -acetyl glucosamine (GlcNAc)	4.0	4.5	n.d.	n.d.	n.d.	n.d.
total carbohydrate	73.5		92.2		111.6	

^a Values are expressed as mole percent of total carbohydrate. ^b n.d.: not detected.

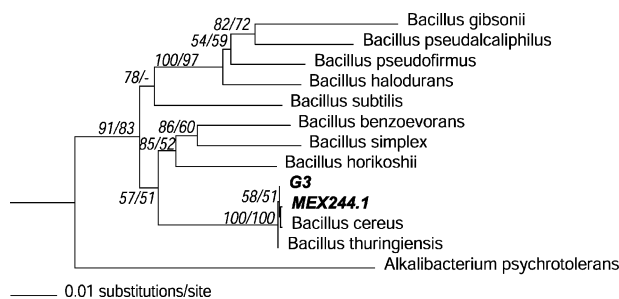


FIGURE 1. Phylogenetic relationships based on partial 16S rDNA sequence (1412 base pairs) of two isolates *MEX244.1* and *G3*. The tree was constructed in PAUP by a neighbor-joining method using Jukes–Cantor corrections. Bootstrap values based on 1000 replicates each (for distance and parsimony) are shown for branches with >50% support. The sequences used for tree construction were submitted to GenBank for *G3* (accession AY987935) and *MEX244.1* (accession AY987936).

from the sampled historic site in Cyprus. *MEX244.1* was selected from a pool of over 200 epilithic biofilm bacteria collected from the Maya site of Ek' Balam in Mexico (27). Amplified 16S rDNA gene sequences were aligned with those of other alkaliphilic *Bacillus* species and microorganisms to identify the isolates (Figure 1). Although the two isolated alkaliphilic microorganisms were phylogenetically very similar, differing in two base positions, they produced EPS with different chemistries (Table 1). The assembled sequence sequences *G3* and *MEX244.1* most closely resembled those of *B. cereus* and *B. thuringiensis*. The relationships of these isolates to other cultured alkaliphilic *Bacillus* species are shown in Figure 1. The EPS of the several isolates also had differing binding capacities for calcite.

EPS produced in culture was harvested from the isolates. The monosaccharide residues and linkages of the EPS samples were analyzed. The EPS samples were large macromolecules with several monosaccharide types (Table 1) and complex branching structures (see Supporting Information). EPS from *G3* was dominantly a polymannose, while EPS from *MEX244.1* and *P. mirabilis* contained larger amounts of other monosaccharides. The detection of glucosamine in the *G3* EPS suggests that the polymer was a part of a glycoprotein. The EPS samples from our isolates had molecular weights of at least 167 kD; this value was used in calculations of molarity. GC-MS chromatograms of the polymers from *G3* and *MEX244.1* had only a single peak, which suggested the presence of a single purified polysaccharide and the absence of contaminating macromolecules. In contrast, the EPS from *P. mirabilis* appeared to have two components (see Supporting Information). The bacteria may also have produced other, smaller oligosaccharides. If such production did occur, either these oligomers were not

collected by the purification procedure or they were present in insignificant quantities in comparison to the large EPS polymer.

Isothermal Titration Calorimetry with Harvested Exopolysaccharides. A suspension of calcite crystals was grown in a supersaturated calcium solution for ITC analysis. The precipitated calcite was predominantly regular (10 $\bar{1}$ 4) rhombohedral crystals. The surface area of the crystals was 0.39 m² g⁻¹ as measured by BET analysis, which was equivalent to 32 × 10⁻³ m² L⁻¹ in the calcite suspension. A similar value was obtained from optical microscopy measurements, indicating that most of the surface area was in the form of large crystals. No evidence of vaterite precipitation was observed by optical microscopy. Filtration of these calcite suspensions resulted in solutions of aqueous calcium. Crystal removal from solutions was confirmed by optical microscopy of multiple samples. This preparation avoided any pH or ionic strength differences between the solutions with and without calcite crystals, which otherwise could have affected the ITC measurements. In solutions with and without calcite crystals, the measured calcium concentration was 0.97 ± 0.03 mM.

ITC measurements were performed for EPS from two natural isolates (*G3* and *MEX244.1*) as well as from *P. mirabilis* Hauser. Experiments were conducted in Nanopure water without calcium, in a solution containing aqueous calcium cations (Ca_(aq)²⁺), and in a solution containing aqueous calcium cations and precipitated calcite (Ca_(aq/surf)²⁺). The titrant contained 1% (w/w) EPS solutions. Heat fluxes accompanying the titrations are shown in Figures 2–4.

Several types of EPS had different heat-flux responses during addition to water (Figure 2). EPS from *MEX244.1* and *P. mirabilis* had very little heat-flux when titrated into water. EPS from *G3* had a slightly exothermic character that stabilized near the baseline, indicating that this biomolecule was very hydrophilic and that energy was released with hydration. For comparison, titration with humic acid (Alfa Aesar, Ward Hill, MA) was also carried out. The heat flux of humic acid was initially endothermic, which possibly resulted from its more hydrophobic nature that requires more energy to successfully disperse in the aqueous milieu. The differences between the observed curves were within the short-term noise range of the ITC (2 nJ s⁻¹).

The differences among the titration profiles may also have resulted from, in part, pH differences of the injectant and calcium/water solutions. The pH values of the calcium/water solutions were as follows: 6.1, 7.8, and 8.0 for Nanopure water, water solutions containing Ca_(aq)²⁺, and water solutions containing Ca_(aq)²⁺ and suspended calcite crystals, respectively. The pH values of the biomolecule titrants also slightly differed: 7.3, 7.0, 6.9, and 6.8 for humic acid, *P. mirabilis* EPS, *G3* EPS, and *MEX244.1* EPS, respectively. The difference

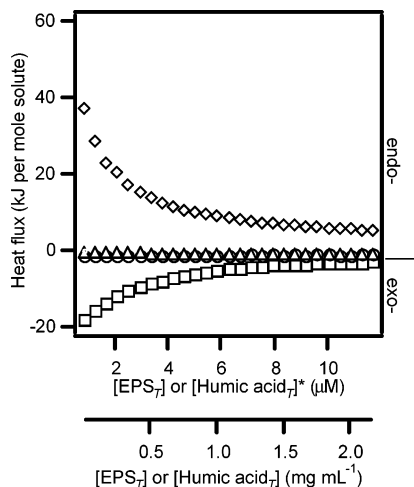


FIGURE 2. Heat flux titration for *G3* EPS (\square), *MEX244.1* EPS (\triangle), *P. mirabilis* EPS (\circ), and humic acid (\diamond). In these experiments, the biomolecule is progressively added to water, so the heat flux arises from the hydration process. *Humic acid molar concentrations are for comparison only because the molecular weight was not determined because of the heterogeneity of the sample.

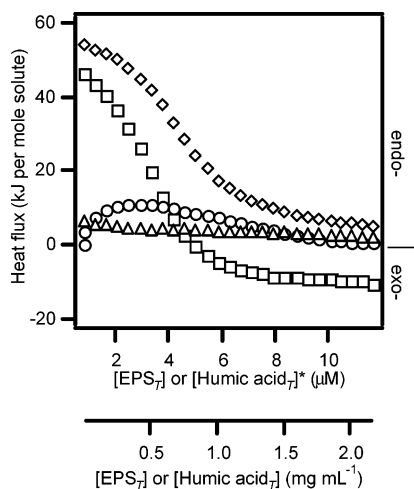


FIGURE 3. Heat flux titration for *G3* EPS (\square), *MEX244.1* EPS (\triangle), *P. mirabilis* EPS (\circ), and humic acid (\diamond). In these experiments, the biomolecule is progressively added to water solutions containing 1 mM $\text{Ca}_{(\text{aq})}^{2+}$, so the heat flux arises from a combination of the H_2O and $\text{Ca}_{(\text{aq})}^{2+}$ binding by the various biomolecules. Induced conformational changes may also contribute to the heat flux.

in pH values of the solutions may affect the magnitude of the recorded results, especially when comparing solutions in the absence and presence of calcium. However, due to the complexity of the acid–base chemistry and conformations of EPS and the similarity of the pH conditions of the solutions containing calcium, we did not adjust the pH or employ buffers. Moreover, solution additives, which otherwise could have affected the EPS adsorption to calcite, were also avoided.

In the next set of experiments, the EPS molecules were titrated into solutions containing aqueous calcium cations. EPS produced by *MEX244.1* was initially slightly endothermic that quickly stabilized at the baseline (Figure 3). We interpreted this behavior as a minimal interaction of the EPS with the aqueous cations, which was caused by a combination of restructuring of the EPS in solution and a breaking of water bonds with EPS and dissolved calcium. Importantly, however, the absolute magnitude of the heat flux was small, which indicated that this polymer weakly associated with calcium ions.

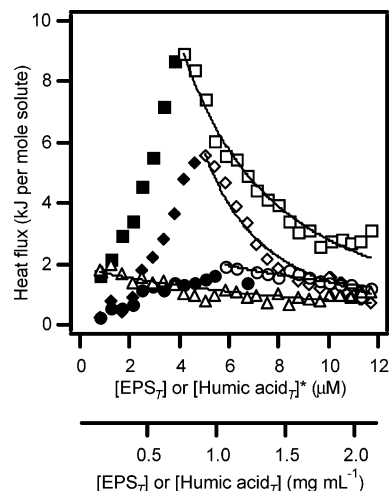


FIGURE 4. Difference in the heat flux in the presence and absence of $\text{CaCO}_{3(\text{s})}$ for (\square/\blacklozenge) *G3* EPS, (\triangle) *MEX244.1* EPS, (\circ/\bullet) *P. mirabilis* EPS, and (\diamond/\blacklozenge) humic acid. These data are determined as the difference of titrations with and without large calcite crystals, so the heat flux arises from $\text{Ca}_{(\text{surf})}^{2+}$ binding by the various biomolecules. In these experiments, the biomolecule is progressively added to water solutions containing 1 mM $\text{Ca}_{(\text{aq})}^{2+}$ and $8.2 \times 10^{-3} \text{ g L}^{-1}$ suspended calcite crystals. Open symbols are the data used for model fitting via a Langmuir type isotherm (lines).

In comparison to *MEX244.1*, EPS from *P. mirabilis* resulted in a mildly more endothermic event (Figure 3), indicating more interaction with the cations. The EPS from *P. mirabilis* stabilizes growing mineral crystals by binding cations (49, 50), which is consistent with our observations of its ability to associate with calcium ions. The initial endothermic nature of this interaction appears counterintuitive when considering normal ligand–receptor energetics, which are often exothermic. Our a priori assumption was that the Coulomb interactions between the positively charged $\text{Ca}_{(\text{aq})}^{2+}$ and a negatively charged, electron-donating oxygen species on the EPS (such as hydroxyls and ethers) would be the driving force for these interactions. The endothermic character of this reaction instead indicated a more important role for the liberation of water from the hydration shells of this hydrophilic EPS (i.e., exoergic but endothermic; cf. Figure 2) (25).

In a final set of experiments, the EPS molecules were titrated into solutions containing suspended calcite crystals. The presence of calcite resulted in an endothermic shift relative to the heat fluxes in the absence of calcite. Direct observation of the heat flux arising from EPS–calcite interactions is complicated by the substantially greater heat flux resulting from EPS hydration and binding of aqueous calcium cations by EPS (25). The heat flux arising from the EPS–calcite interaction can, however, be obtained by taking the difference of the heat flux into calcite suspensions from the heat flux in filtered solutions. The resulting heat flux is shown in Figure 4.

Figure 4 shows that the heat flux associated with surface binding by EPS from *G3* became increasingly endothermic but then abruptly switched to increasingly exothermic during the reaction. The data profiles show an increasingly endothermic behavior for $0 < [\text{EPS}] < 4\text{--}6 \mu\text{M}$ followed by an increasingly exothermic behavior for $[\text{EPS}] > 6 \mu\text{M}$. These data suggest that, for $[\text{EPS}] < 4\text{--}6 \mu\text{M}$, EPS from *G3* preferentially binds to aqueous cations first due to the greater effect of hydration shell disruption when binding aqueous cations as compared to surficial cations. For $[\text{EPS}] < 4\text{--}6 \mu\text{M}$, the concentration of the reactive sites on the EPS approximates the concentration of aqueous cations. Once EPS has bound the aqueous calcium (e.g., $4\text{--}6 \mu\text{M}$), it begins to bind to the calcite surface. The inflection point in Figure

4 shows the crossover during the titrations. This behavior is similarly observed for the humic acid–calcite interaction, although the magnitude of the heat flux resulting from the reaction diminishes. The ability of the EPS to scavenge cations appears to be a relatively fast process that binds the aqueous calcium faster than it is replaced by accelerated dissolution of the calcite crystal through lowering of aqueous saturation (21). The descending portion of the data for $[\text{EPS}_{\text{T}}] > 4 \mu\text{M}$ is attributed to the binding of calcite reactive surface sites by EPS and eventual surface equilibrium. In comparison to EPS from G3, EPS from *P. mirabilis* and MEX244.1 had weak interactions (i.e., small heat flux) with the calcite surface.

We developed a calcium-binding mass balance from information about the G3 polymer structure (viz. Table 1). It showed that for $[\text{EPS}_{\text{T}}] < 4\text{--}6 \mu\text{M}$, the concentration of EPS reactive sites approximates the number of aqueous calcium ions. Chemical characterization of the polymer permits estimation of the maximum calcium binding capacity $(\text{EPS} \cdot \text{Ca}^{2+})_{\text{max}}$ per mole of polymer via

$$(\text{EPS} \cdot \text{Ca}^{2+})_{\text{max}} = \left(\frac{\text{MW}_{\text{EPS}}}{i_6 \text{MW}_6 + i_5 \text{MW}_5} \right) / q \quad (1)$$

where MW_{EPS} is the molecular weight of the EPS, MW_6 and MW_5 are the average molecular weights of the six- and five-membered monosaccharides detected, i_6 and i_5 are their percent contributions, and q is the coordination of the binding reaction. This equation estimates the number of cation binding sites from the relative fractions of detected five- and six-membered sugar rings. We assume octadentate coordination of EPS monosaccharides around a single calcium ion because this coordination has been observed as a maximum binding capability for other natural polymers (51). The calculated result is that EPS produced by G3 binds 220 mol of calcium per mol of polymer. For $[\text{EPS}_{\text{T}}] = 4 \mu\text{M}$, the concentration of octadentate reactive sites on G3 approximates the concentration of aqueous cations. This calculation supports the earlier statement of the role of aqueous calcite EPS binding in the ascending portion of the heat-flux data (Figure 4).

Langmuir Binding Model. A two-parameter Langmuir model can be fit to the data to determine an adsorption constant (K_{ads}) and specific enthalpy (ΔH_{surf}) for the EPS–calcite interactions, as defined in eq 8 of the Supporting Information. A Langmuir-type isotherm (25), a commonly used descriptor of surface adsorption, is used to explain the adsorption of the biomolecule to the calcite surface. The model assumes that there is a single type of reaction site on both biomolecule and calcite. This simplification of the system, in which both reactive species are heterogeneous due to complex monosaccharide arrangements and branching structures of EPS and the complex surficial features on calcite, is nevertheless valuable for quantification of the EPS–calcite interaction and adequately accounts for the empirical results.

The Langmuir model is applied only to later injections (after the inflection point) because chelation of aqueous cations affects the heat flux in the early injections of the titration. Model-fit lines are shown in Figure 4. The fitted values for the adsorption constants and enthalpy are given in Table 2 for EPS from G3, MEX244.1, *P. mirabilis*, and humic acid.

Environmental Implications. Alkaliphilic bacteria are often the primary colonizers of fresh limestone surfaces. A freshly exposed calcite mineral surface under aqueous conditions has a pH of 8–10 (26), which naturally enriches for alkaliphilic or alkalitolerant bacteria. These initial colonizers produce metabolic byproducts, such as EPS. These byproducts may contribute to early dissolution processes during biofilm development (11, 21). The bacteria have the

TABLE 2. Fitted Parameters for Biomolecule Reactions with Calcite

macromolecule	$K_{\text{ads}} (\text{M}^{-1})$	$\Delta H_{\text{surf}} (\text{J m}^{-2})$	R^2
G3 EPS	1.52×10^5	2.33	0.99
MEX244.1 EPS	5.25×10^4	1.12	0.82
<i>P. mirabilis</i> EPS	5.00×10^4	1.33	0.95
humic acid ^a	3.00×10^5	0.99	0.99

^a Humic acid values are for comparison only because molecular weight was not determined due to the heterogeneity of the sample.

metabolic ability to produce different EPS depending on growth stage, nutrient conditions, and other environmental factors, which will have different dissolution effects.

Nonpolar electron-donating groups are important in stabilizing the EPS–calcium complex. The EPS monosaccharide residues detected in our study are a mixture of five- and six-membered sugars without reactive moieties that would typically be implicated in a reaction with a polar mineral surface, such as carboxylates. However, carboxylates are absent on the monosaccharides detected in the harvested EPS. The absence of these moieties indicates that hydration of the polymer, rather than Coulombic interactions, may be the driving force for surface adsorption (25) and that the role of hydroxyls and linkage esters in binding to a mineral surface is significant.

In natural environments, biological macromolecules such as EPS may play an underestimated role in dissolution reactions. Humic acids are abundant organic species that play a role in mineral weathering (17, 18). However, EPS polysaccharides are also abundant biopolymers. The observation that EPS can have different binding interactions with calcite and that the effect can be of similar magnitude to that of humic acid indicates that these polymers should be considered when modeling mineral weathering (19).

Acknowledgments

TDP was supported by a Sandia National Laboratories Campus Executive Fellowship. This work was funded in part by support from the U.S. Department of Energy to S.T.M., the N.S.F. to M.F.P., and the W. R. Grace Corporation to R.M. Microbial samples from Cyprus were collected by M. Breuker, National Parks Service. The authors thank Drs. V. Frasca and L.-N. Lin of MicroCal (Northampton, MA) for their contributions to the isothermal titration calorimetry. Polysaccharide analysis was performed at the Department of Energy-Funded (DE-FG09-93ER-20097) Center for Plant and Microbial Complex Carbohydrates. BET analysis was performed at Quantachrome Instruments, Boynton Beach, FL.

Supporting Information Available

Tabulated data of glycosyl linkage analysis of different EPS molecules and derivation and application of the kinetic binding model. This material is available free of charge via the Internet at <http://pubs.acs.org>.

Literature Cited

- Schlesinger, W. H. *Biogeochemistry: An Analysis of Global Change*, 2nd ed.; Academic Press: San Diego, 1997.
- Pilson, M. *An Introduction to the Chemistry of the Sea*; Prentice Hall: Upper Saddle River, NJ, 1998.
- Stumm, W. *Chemistry of the Solid–Water Interface*; Wiley: New York, 1992.
- Stumm, W.; Morgan, J. J. *Aquatic Chemistry*, 3rd ed.; Wiley: New York, 1996.
- Amirbahman, A.; Schoenberger, R.; Johnson, C.; Sigg, L. Aqueous- and solid-phase biogeochemistry of a calcareous aquifer system downgradient from a municipal solid waste landfill (Winterthur, Switzerland). *Environ. Sci. Technol.* **1998**, *32*, 1933–1940.

- (6) Saiz-Jimenez, C. Biogeochemistry of weathering processes in monuments. *Geomicrobiol. J.* **1999**, *16*, 27–37.
- (7) Ochs, M. Influence of humified and nonhumified natural organic compounds on mineral dissolution. *Chem. Geol.* **1996**, *132*, 119–124.
- (8) Arvidson, R. S.; Ertan, I. E.; Amonette, J. E.; Luttge, A. Variation in calcite dissolution rates: A fundamental problem? *Geochim. Cosmochim. Acta* **2003**, *67*, 1623–1634.
- (9) Christensen, B. E.; Charaklis, W. G. In *Biofilms*; Charaklis, W. G., Marshall, K. C., Eds.; Wiley: New York, 1990.
- (10) Sand, W. Microbial mechanisms of deterioration of inorganic substrates—A general mechanistic overview. *Int. Biodeterior. Biodegrad.* **1997**, *40*, 183–190.
- (11) Perry, T. D., IV; McNamara, C. J.; Mitchell, R. In *Scientific Examination of Art: Modern Techniques in Conservation and Analysis*; National Academy of Science Press: Washington, DC, 2005.
- (12) Suess, E. Interaction of organic compounds with calcium carbonate I. Associated phenomena and geochemical implications. *Geochim. Cosmochim. Acta* **1970**, *34*, 157–168.
- (13) Frye, G.; Thomas, M. Adsorption of organic compounds on carbonate minerals 2. Extraction of carboxylic acids from recent and ancient carbonates. *Chem. Geol.* **1993**, *109*, 215–226.
- (14) Hoch, A.; Reddy, M.; Aiken, G. Calcite crystal growth by humic substances with emphasis on hydrophobic acids from the everglades. *Geochim. Cosmochim. Acta* **2000**, *64*, 61–72.
- (15) Fredd, C.; Fogler, H. The influence of chelating agents on the kinetics of calcite dissolution. *J. Colloid Interface Sci.* **1998**, *204*, 187–194.
- (16) Wu, Y.; Grant, C. Effect of chelation chemistry of sodium polyaspartate on the dissolution of calcite. *Langmuir* **2002**, *18*, 6813–6820.
- (17) Thomas, M.; Clouse, J.; Longo, J. Adsorption of organic compounds on carbonate minerals 3. Influence on dissolution rates. *Chem. Geol.* **1993**, *109*, 227–237.
- (18) Compton, R. G.; Sanders, G. The dissolution of calcite in aqueous acid: The influence of humic species. *J. Colloid Interface Sci.* **1993**, *158*, 439–445.
- (19) Barker, W. W.; Banfield, J. F. Biologically versus inorganically mediated weathering reaction: relationships between mineral and extracellular microbial polymers in lithobiontic communities. *Chem. Geol.* **1996**, *132*, 55–69.
- (20) Barker, W. W.; Welch, S. A.; Banfield, J. F. In *Geomicrobiology: Interactions between Microbes and Minerals*; Banfield, J. F., Nealson, K. H., Eds.; Mineralogical Society of America: Washington, DC, 1997; Vol. 35, pp 391–428.
- (21) Perry, T. D., IV; Duckworth, O. W.; McNamara, C. J.; Martin, S. T.; Mitchell, R. Effects of the biologically produced polymer alginate on macroscopic and microscopic calcite dissolution rates. *Environ. Sci. Technol.* **2004**, *38*, 3040–3046.
- (22) Welch, S. A.; Vandevivere, P. Effect of microbial and other naturally occurring polymers on mineral dissolution. *Geomicrobiol. J.* **1994**, *12*, 227–238.
- (23) Banfield, J. F.; Barker, W. W.; Welch, S. A.; Taunton, A. Biological impact on mineral dissolution: Application of the lichen model to understanding mineral weathering in the rhizosphere. *Proc. Natl. Acad. Sci. U.S.A.* **1999**, *96*, 3404–3411.
- (24) Flemming, H. C.; Wingender, J. Relevance of microbial extracellular polymeric substances (EPSs) Part II: Technical aspects. *Water Sci. Technol.* **2001**, *43*, 9–16.
- (25) Dimova, R.; Lipowsky, R.; Mastai, Y.; Antonietti, M. Binding of polymers to calcite crystals in water: Characterization by isothermal titration calorimetry. *Langmuir* **2003**, *19*, 6097–6103.
- (26) Horikoshi, K. In *Extremophiles; microbial life in extreme environments*; Horikoshi, K., Grant, W. D., Eds.; Wiley-Liss: New York, 1998; pp 155–180.
- (27) McNamara, C. J.; Perry, T. D.; Bearce, K.; Hernandez-Duque, G.; Mitchell, R. Epilithic and endolithic bacterial communities in limestone from a Maya archaeological site. *Microbiol. Ecol.*, in press.
- (28) Di Bonaventura, M. P.; Gallo, M. D.; Cacchio, P.; Ercole, C.; Lepidi, A. Microbial formation of oxalate films on monument surfaces: bioprotection or biodeterioration? *Geomicrobiol. J.* **1999**, *16*, 55–64.
- (29) Lane, D. J. In *Neucleic Acid Techniques in Bacterial Systematics*; Stackebrandt, E., Goodfellow, M., Eds.; John Wiley & Sons: Chichester, 1991; pp 115–148.
- (30) Schabereiter-Gurtner, C.; Pinar, G.; Lubitz, W.; Rolleke, S. An advanced molecular strategy to identify bacterial communities on art objects. *J. Microbiol. Methods* **2001**, *45*, 77–87.
- (31) Cannone, J. J.; Subramanian, S.; Schnare, M. N.; Collett, J. R.; D'Souza, L. M.; Du, Y.; Feng, B.; Lin, N.; Madabus, L. V.; Müller, K. M.; Pande, N.; Shang, Z.; Yu, N.; Gutell, R. R. The Comparative RNA Web (CRW) Site: An Online Database of Comparative Sequence and Structure Information for Ribosomal, Intron, and other RNAs. *BioMed. Central. Bioinf.* **2002**, *3*.
- (32) Cole, J.; Chai, B.; Farris, R.; Wang, Q.; Kulam, S.; McGarrell, D.; Garrity, G.; Tiedje, J. The Ribosomal Database Project (RDP-II): sequences and tools for high-throughput rRNA analysis. *Nucleic Acids Res.* **2005**, *1*.
- (33) Altschul, S.; Madden, T.; Schaffer, A.; Zhang, J.; Zhang, Z.; Miller, W.; Lipman, D. Gapped BLAST and PSI-BLAST: a new generation of protein database search programs. *Nucl. Acids Res.* **1997**, *25*, 3389–3402.
- (34) Maidak, B. L.; Olsen, G. J.; Larsen, N.; Overbeek, R.; McCaughey, M. J.; Woese, C. R. The RDP (Ribosomal Database Project). *Nucleic Acids Res.* **1999**, *25*.
- (35) Maidak, B. L.; Cole, J. R.; Lilburn, T. G.; Parker, C. T.; Saxman, P. R.; Farris, R. J.; Garrity, G. M.; Olsen, G. J.; Schmidt, T. M.; Tiedje, J. M. The RDP-II (Ribosomal Database Project). *Nucleic Acids Res.* **2001**, *29*, 173–174.
- (36) Swofford, D. L. PAUP—a computer program for phylogenetic inference using maximum parsimony. *J. Gen. Physiol.* **1993**, *102*, A9.
- (37) Gonçalves, V.; Takagi, M.; Lima, R.; Massaldi, H.; Giordano, R.; Tanizaki, M. Purification of capsular polysaccharide from *Streptococcus pneumoniae* serotype 23F by a procedure suitable for scale-up. *Biotechnol. Appl. Biochem.* **2003**, *37*, 283–287.
- (38) York, W. S.; Darvill, A. G.; McNeil, M.; Stevenson, T. T.; Albersheim, P. In *Methods in Enzymology*; Colowick, S. P., Kaplan, N. O., Eds.; Academic Press: New York, 1985; Vol. 118, pp 3–40.
- (39) Ciucanu, I.; Kerek, F. A simple and rapid method for the permethylation of carbohydrates. *Carbohydr. Res.* **1984**, *131*, 209–217.
- (40) Kitano, Y.; Hood, D. W.; Park, K. Pure aragonite synthesis. *J. Geophys. Res.* **1962**, *67*, 4873.
- (41) Rudloff, J.; Antonietti, M.; Colfen, H.; Pretula, J.; Kaluzynski, K.; Penczek, S. Double-hydrophilic block copolymers with monophosphate ester moieties as crystal growth modifiers of CaCO₃. *Macromol. Chem. Phys.* **2002**, *203*, 627–635.
- (42) Duckworth, O. W.; Martin, S. T. Dissolution rates and pit morphologies of rhombohedral carbonate minerals. *Am. Mineral.* **2004**, *89*, 554–563.
- (43) Shiraki, R.; Rock, P. A.; Casey, W. H. Dissolution kinetics of calcite in 0.1 M NaCl solution at room temperature: An atomic force microscopic (AFM) study. *Aquat. Geochem.* **2000**, *6*, 87–108.
- (44) Kudo, T.; Horikoshi, K. Effect of pH and sodium ion on fermentation of alkaliphilic *Bacillus* species. *Agric. Biol. Chem.* **1983**, *47*, 665–669.
- (45) Boyer, E. W.; Ingle, M. B.; Mercer, G. D. *Bacillus alcalophilus* subsp. *halodurans* subsp. nov: an alkaline-amylose producing alkaliphilic organism. *Int. J. Systematic Bacteriol.* **1973**, *50*, 697–703.
- (46) Krulwich, T. A.; Ito, M.; Guffanti, A. A. The Na⁺-dependence of alkaliphilicity in *Bacillus*. *Biochim. Biophys. Acta* **2001**, *1505*, 158–168.
- (47) Personal communication: M. Breuker, 2005, National Park Service.
- (48) McNamara, C. J.; Bearce, K.; Perry, T. D., IV; Mitchell, R. Measurement of limestone biodeterioration using the Ca²⁺ binding fluorochrome Rhod-5N. *J. Microbiol. Methods* **2005**, *61*, 245–250.
- (49) Clapham, I.; McLean, R.; Nickel, L.; Downey, J.; Costerton, J. The influence of bacteria on struvite crystal habit and its importance in urinary stone formation. *J. Cryst. Growth* **1990**, *104*, 475–484.
- (50) Dumanski, A.; Hedelin, H.; Edin-Liljegren, A.; Beauchemin, D.; McLean, R. J. C. Unique ability of *Proteus mirabilis* capsule to enhance mineral growth in infectious urinary calculi. *Infect. Immun.* **1994**, *62*, 2998–3003.
- (51) Gregor, J. E.; Fenton, E.; Brokenshire, G.; VandenBrink, P.; Osullivan, B. Interactions of calcium and aluminium ions with alginate. *Water Res.* **1996**, *30*, 1319–1324.

Received for review May 2, 2005. Revised manuscript received August 5, 2005. Accepted August 12, 2005.

ES0508368